

## 香豆素衍生物荧光传感器对 $Zn^{2+}$ 的识别及细胞成像

尹计秋<sup>1,2</sup> 安永林<sup>1</sup> 贾献超<sup>1</sup> 焦扬<sup>\*1</sup>

(<sup>1</sup>大连理工大学精细化工国家重点实验室,大连 116024)

(<sup>2</sup>大连医科大学检验医学院,大连 116044)

**摘要:** 制备了基于香豆素衍生物的荧光传感器CANQ,其可选择性地识别  $Zn^{2+}$  离子。通过NMR、MS、荧光光谱等技术研究了传感器的结构及荧光性能。传感器CANQ对  $Zn^{2+}$  离子具有显著的荧光增强响应,且响应速度快、选择性高、生物相容性好,可用于MCF-7细胞中  $Zn^{2+}$  离子的成像。

**关键词:**  $Zn^{2+}$  离子; 香豆素衍生物; 荧光传感器; 识别

中图分类号: O614.24<sup>+1</sup> 文献标识码: A 文章编号: 1001-4861(2022)02-0368-09

DOI: 10.11862/CJIC.2022.039

## Recognition and Cell Imaging of $Zn^{2+}$ by Coumarin Derivative Fluorescence Sensor

YIN Ji-Qiu<sup>1,2</sup> AN Yong-Lin<sup>1</sup> JIA Xian-Chao<sup>1</sup> JIAO Yang<sup>\*1</sup>

(<sup>1</sup>State Key Laboratory of Fine Chemicals, Dalian University of Technology, Dalian, Liaoning 116024, China)

(<sup>2</sup>College of Medical Laboratory, Dalian Medical University, Dalian, Liaoning 116044, China)

**Abstract:** Coumarin-derived fluorescence sensor was designed and synthesized to selectively recognize  $Zn^{2+}$  ions. The structure and fluorescence properties of the sensor were investigated by NMR, MS, fluorescence spectroscopy, and other technical methods. Sensor CANQ exhibited conspicuous fluorescent enhancement response to  $Zn^{2+}$  ion and had the characteristic of fast response, high selectivity, and good biocompatibility. It has been applied to the imaging of  $Zn^{2+}$  ions in MCF-7 cells.

**Keywords:**  $Zn^{2+}$  ion; coumarin derivative; fluorescent sensor; recognition

### 0 Introduction

Trace elements play an important physiological function in the life activities of the organism and they are involved in the synthesis of biological macromolecules such as enzymes, hormones, and vitamins<sup>[1-3]</sup>. Zinc, which is an essential trace element in the body, is the second most abundant transition metal ion in the human body and the concentration of zinc in human plasma is above  $10 \mu\text{mol}\cdot\text{L}^{-1}$ , its content in the human body is only less than iron<sup>[4-7]</sup>. Zinc participates in physiological processes such as neurotransmitter transmis-

sion, gene expression, enzyme activity, and DNA synthesis, which plays a key role in a variety of biological processes<sup>[8-9]</sup>. Zinc metabolism imbalance will cause a series of pathological changes and eventually lead to diseases and apoptosis, such as Alzheimer's and Parkinson's diseases<sup>[10-12]</sup>. The decrease of enzyme function related to zinc and the regulation failure of biological signals are crucial factors in the occurrence and development of tumors<sup>[13]</sup>. Moreover, zinc is also widely applied in industrial, large amounts of  $Zn^{2+}$  ions enter the water and soil, which have adverse effects on aquatic

收稿日期:2021-07-30。收修改稿日期:2021-11-17。

大连市高层次人才创新支持计划(No.2019RQ039)和中央高校基本科研业务费专项资金(No.DUT20LK12)资助。

\*通信联系人。E-mail: jiaoyang@dlut.edu.cn

organisms and soil microorganisms to lead environmental pollutants. Therefore, rapid and effective identification and detection of  $Zn^{2+}$  ions are of great significance to the diagnosis of related diseases, environmental pollution monitoring, and other research fields.

Compared with traditional methods (inductively coupled plasma mass spectrometry, atomic absorption spectroscopy, and electrochemistry) for detecting  $Zn^{2+}$  ions<sup>[14-17]</sup>, the fluorescent detection method has advantages of simple operation, low cost, high sensitivity, specific selectivity, and real-time detection, *etc.* It is favored by researchers with the suitable characteristic for direct imaging and biosensors and is currently the relatively superior assay method for  $Zn^{2+}$  ions in living cells<sup>[18-24]</sup>. In recent years, fluorescent sensors for detecting  $Zn^{2+}$  ions were widely reported based on different fluorophores, such as rhodamine, fluorescein, BODIPY (boron dipyrromethene), cyanine, oxazoline<sup>[25-31]</sup>. It is one of the current research hotspots of developing fluorescence sensors with high sensitivity and high selectivity to monitor  $Zn^{2+}$  in biological and environmental systems.

Coumarin is a kind of lactone compound with a benzo  $\alpha$ -pyrone core, and coumarin derivatives have good fluorescence properties with a wide application as fluorescent dyes<sup>[32]</sup>. Coumarin derivatives contain C=C, C=O, and lactone in their parent ring benzopyranes, which enhance the conjugation level and rigidity of the molecular system, and they have high fluorescence quantum yields, large Stokes shifts, and good photochemical stability<sup>[33-37]</sup>. Coumarin fluorophore is an ideal model for constructing fluorescent chemical sensors recognizing  $Zn^{2+}$  ion<sup>[38-41]</sup> and coumarin ring can be modified by hydroxyl, alkoxy, isoprene, carbonyl, and other substituents. Coumarin derivatives are often used in the detection of common metal ions and small molecules, and the colorimetric and fluorescent sensor provides a highly accurate quantitative analysis<sup>[42-44]</sup>. Coumarin derivatives have biological activities (anti-cancer, anti-oxidation, and inhibiting tyrosinase<sup>[45-47]</sup>) and high biocompatibility, fluorescent sensors based on coumarin derivatives have a broad prospect in the detection of metal ions in a biological system. Further-

more, quinoxaline derivative is a heterocyclic compound containing one nitrogen atom and the synthesis methods of quinoxaline derivative is an efficient, simple, and green procedure. Acenaphthene quinone is usually used as raw material at a low cost. Quinoxaline derivative is of potent biological activities and fluorescence emission of quinoxaline derivative can be easily distinguished from the environment of cells, which has been widely used in tumor cell imaging<sup>[48-50]</sup>.

Herein, a fluorescent sensor was designed based on coumarin derivative to realize the purpose of  $Zn^{2+}$  ion detection. Coumarin aldehyde derivative reacted with the amino compound by forming a Schiff base to introduce quinoxaline derivatives into the design of sensor CANQ. The fluorescent sensor CANQ could selectively recognize  $Zn^{2+}$  ion in  $CH_3CH_2OH/Tris-HCl$  solution and the fluorescence intensity of sensor CANQ gradually enhance with the adding of  $Zn^{2+}$  ion. Sensor CANQ was applied to MCF-7 cell biological imaging, which verified the possibility of sensor CANQ imaging application.

## 1 Experimental

### 1.1 Materials and instruments

All chemical reagents were obtained from commercial sources and used without further purification except the solvents which were purified by classical methods. DMEM medium and fetal bovine serum (FBS) were purchased from Invitrogen. The reactions were monitored by TLC and were observed by a handheld UV analyzer (254 and 365 nm).  $^1H$  NMR spectra were measured on a Bruker AVANCE III 400 MHz NMR spectrometer and Varian DLG 400 MHz NMR spectrometer. Mass spectrometry was carried out on a Thermo Scientific-LTQ Orbitrap XL spectrometer and UPLC-Q-TOF MS. The fluorescence spectra were recorded by the FS920 fluorescence spectrometer. The absorbances of the CCK-8 assay were measured by BIORAD xMark Microplate Spectrophotometer. Confocal imaging of cells was recorded with OLYMPUS FV1000 confocal microscopy.

### 1.2 Synthesis

The fluorescence sensor CANQ was synthesized

by a five-step reaction. The detailed synthetic steps are shown in Scheme 1.

### 1.2.1 Synthesis of compound **1**<sup>[51]</sup>

4-Diethylaminosalicylic aldehyde (1.93 g, 10 mmol) and diethyl malonate (3.2 g, 20 mmol) were mixed in an ethanol solution (30 mL). 1 mL piperidine was added under stirring and the solution was refluxed for 6 h. After ethanol was removed by vacuum distillation, 20 mL concentrated hydrochloric acid and 20 mL glacial acetic acid were added and stirred for 6 h. The reaction solution was cooled down to room temperature and was poured into 100 mL ice water. The pH value was adjusted to 5 with sodium hydroxide and the gray precipitation formed gradually. The solid was filtered and the crude product was recrystallized from toluene to obtain 1.70 g compound **1** (Yield: 78.3%). <sup>1</sup>H NMR (400 MHz, CDCl<sub>3</sub>): δ 7.53 (d, *J*=9.3 Hz, 1H), 7.24 (d, *J*=8.8 Hz, 1H), 6.56 (dd, *J*=8.8, 2.3 Hz, 1H), 6.48 (d, *J*=2.1 Hz, 1H), 6.03 (d, *J*=9.3 Hz, 1H), 3.41 (q, *J*=7.1 Hz, 4H), 1.21 (t, *J*=7.1 Hz, 6H). HRMS: *m/z* Calcd. for [C<sub>13</sub>H<sub>15</sub>NO<sub>2</sub>+H]<sup>+</sup> 218.117 6; Obs. 218.117 5.

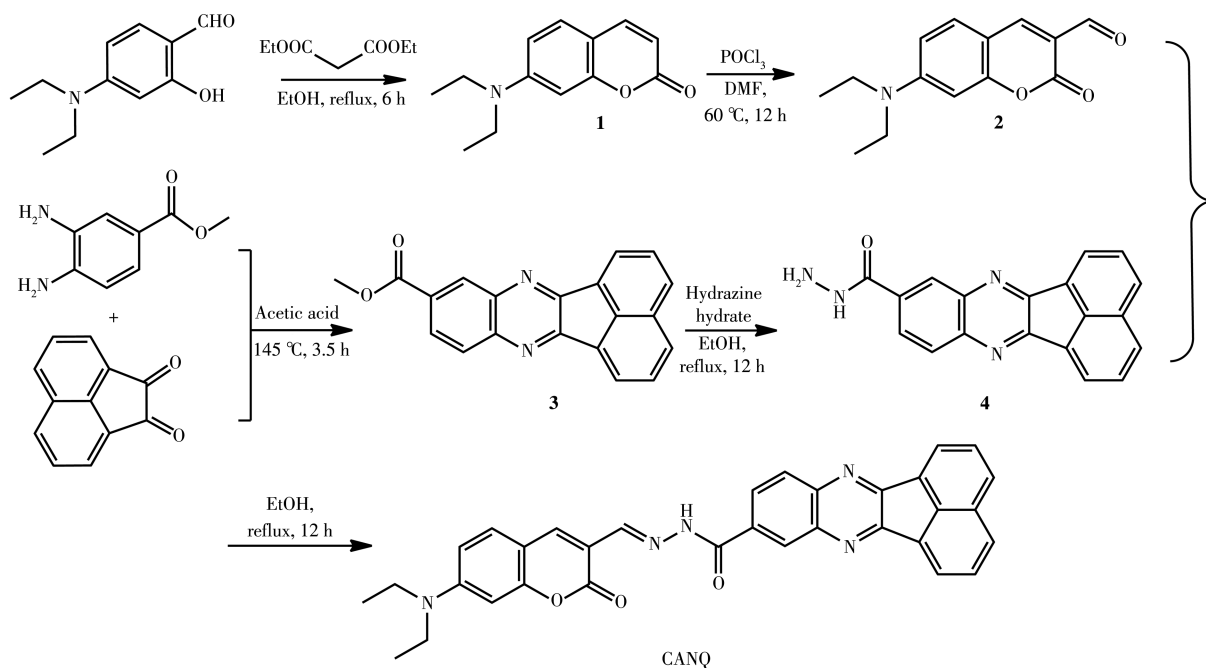
### 1.2.2 Synthesis of compound **2**<sup>[52]</sup>

POCl<sub>3</sub> (4 mL) was added to 4 mL *N,N*-dimethylformamide (DMF) dropwise in an ice bath and stirred for 30 min at room temperature under an argon atmo-

sphere. 3 g (13.8 mmol) compound **1** was dissolved into 20 mL DMF, and the solution was slowly added into the DMF solution containing POCl<sub>3</sub>. The reaction solution was stirred for 12 h at 60 °C. Then the solution was poured into 200 mL ice water, and NaOH solution (20%) was added dropwise to adjust the pH value to 7. The obtained orange precipitate was filtered and washed with water several times. The crude product was dried, and was separated and purified by column chromatography. 1.9 g compound **2** was obtained (Yield: 56.2%). <sup>1</sup>H NMR (400 MHz, CDCl<sub>3</sub>): δ 10.11 (s, 1H), 8.25 (s, 1H), 7.41 (d, *J*=9.0 Hz, 1H), 6.64 (dd, *J*=9.0, 2.5 Hz, 1H), 6.48 (d, *J*=2.3 Hz, 1H), 3.48 (q, *J*=7.1 Hz, 4H), 1.26 (t, *J*=7.1 Hz, 6H). HRMS: *m/z* Calcd. for [C<sub>14</sub>H<sub>15</sub>NO<sub>3</sub>+H]<sup>+</sup> 246.112 5; Obs. 246.112 7.

### 1.2.3 Synthesis of compound **3**<sup>[53]</sup>

Acenaphthylene-1,2-dione (182 mg, 1.0 mmol) and methyl 3,4-diaminobenzoate (216 mg, 1.3 mmol) were taken into a 100 mL round-bottom flask, and 50 mL glacial acetic acid was added to dissolve them. The solution was heated to 145 °C and was refluxed for 3.5 h. After the reaction was cooled, the precipitate formed. The solid was filtered and the crude product was recrystallized from DMF. After most of the solids were separated, suction filtration was performed, and a



Scheme 1 Synthesis route of CANQ

small amount of methanol and ether was added for washing. 158 mg compound **3** was obtained (Yield: 50.6%). <sup>1</sup>H NMR (400 MHz, CDCl<sub>3</sub>): δ 8.83 (d, *J*=1.8 Hz, 1H), 8.35 (dd, *J*=6.9, 2.3 Hz, 2H), 8.28 (dd, *J*=8.6, 1.9 Hz, 1H), 8.15 (d, *J*=8.6 Hz, 1H), 8.08-8.04 (m, 2H), 7.80 (dd, *J*=8.1, 7.2 Hz, 2H), 4.02 (s, 3H). HRMS: *m/z* Calcd. for [C<sub>20</sub>H<sub>12</sub>N<sub>2</sub>O<sub>2</sub>+H]<sup>+</sup> 313.097 2; Obs. 313.097 3.

#### 1.2.4 Synthesis of compound **4**<sup>[54]</sup>

Compound **3** (312 mg, 1 mmol) was dissolved in 15 mL ethanol. 1 mL 80% hydrazine hydrate was added dropwise and the mixture solution was stirred and refluxed for 12 h. After cooling and standing in an ice bath for 2 h, the mixture was filtered. The solid was washed with cold ethanol (20 mL×3), and was dried to obtain 187 mg compound **4** (Yield: 59.9%). <sup>1</sup>H NMR (400 MHz, DMSO-*d*<sub>6</sub>): δ 10.17 (s, 1H), 8.68 (d, *J*=1.5 Hz, 1H), 8.49 (d, *J*=6.9 Hz, 2H), 8.36 (dd, *J*=8.2, 1.7 Hz, 2H), 8.28 (d, *J*=8.5 Hz, 1H), 8.26-8.22 (m, 1H), 8.02-7.96 (m, 2H), 4.66 (s, 2H). HRMS: *m/z* Calcd. for [C<sub>19</sub>H<sub>12</sub>N<sub>4</sub>O+H]<sup>+</sup> 313.108 4; Obs. 313.107 1.

#### 1.2.5 Synthesis of compound CANQ

Compound **2** (245 mg, 1 mmol) was dissolved in 50 mL ethanol and stirred, then compound **4** (312 mg, 1 mmol) was added, and 3-5 drops of glacial acetic acid were added. The reaction was refluxed for 12 h. After the reaction was completed, the solution was cooled to 0 °C to form precipitate. After filtration, the solid was washed with cold ethanol (20 mL×3) and dried to obtain 432 mg CANQ (Yield: 80.1%). <sup>1</sup>H NMR (400 MHz, DMSO-*d*<sub>6</sub>): δ 12.21 (s, 1H), 8.84 (s, 1H), 8.59 (s, 1H), 8.48-8.43 (m, 2H), 8.37 (s, 1H), 8.34 (d, *J*=8.3 Hz, 2H), 8.31 (s, 2H), 8.01-7.93(m, 2H), 7.63 (d, *J*=8.9 Hz, 1H), 6.73 (d, *J*=8.8 Hz, 1H), 6.55 (s, 1H), 3.53-3.46 (m, 4H), 1.14 (t, *J*=6.9 Hz, 6H). HRMS: *m/z* Calcd. for [C<sub>33</sub>H<sub>25</sub>N<sub>5</sub>O<sub>3</sub>+Na]<sup>+</sup> 562.185 0, Obs. 562.183 2.

### 1.3 Fluorescence measurements

The sensor CANQ stock solution was prepared with dimethyl sulfoxide (DMSO) to a concentration of 1 mmol·L<sup>-1</sup>. The CANQ stock solution was diluted to obtain 5.0 μmol·L<sup>-1</sup> with CH<sub>3</sub>CH<sub>2</sub>OH/Tris-HCl (8:2, *V/V*) solution (Tris-HCl: 20 mmol·L<sup>-1</sup>, pH=7.4) and fluorescent spectrum scanning was performed. Perchlorate stock solutions (0.01 mol·L<sup>-1</sup>) of various metal ions (including the perchlorate of Pb<sup>2+</sup>, Na<sup>+</sup>, Mn<sup>2+</sup>, Ca<sup>2+</sup>,

Mg<sup>2+</sup>, Ag<sup>+</sup>, Cr<sup>3+</sup>, Fe<sup>3+</sup>, Fe<sup>2+</sup>, Hg<sup>2+</sup>, K<sup>+</sup>, Cd<sup>2+</sup>, Al<sup>3+</sup>, Cu<sup>2+</sup>, Zn<sup>2+</sup>) were prepared with deionized water. The excitation wavelength was 468 nm, the emission wavelength was 522 nm, and the slit width was 2.5 nm.

### 1.4 Cytotoxicity assay

MCF-7 cells were seeded in 96 well plates. After the cells adhered to the wall, different concentrations (0, 1, 2, 5, 10, and 20 μmol·L<sup>-1</sup>) of sensor CANQ were added to the cell culture medium and incubated for 24 h in 5% volume fraction of CO<sub>2</sub> at 37 °C. CCK-8 solution was added to each orifice and incubated on the culture plate for 1 h. The absorbance at 450 nm was determined by an enzyme marker and relative cell viability (*f*<sub>CV</sub>) was calculated using the equation by Graphpad prism soft:  $f_{CV} = (A_s - A_b) / (A_c - A_b) \times 100\%$ , where *A*<sub>s</sub>, *A*<sub>c</sub>, and *A*<sub>b</sub> represent the absorbance of sensor-treated cells, the absorbance of control cells, and the absorbance of the blank solution, respectively.

### 1.5 Cell culture and confocal imaging

MCF-7 cells were cultured in a DMEM medium containing 10% FBS in a 5% volume fraction of CO<sub>2</sub> at 37 °C. MCF-7 cells were inoculated into confocal dishes and cells were incubated in the culture medium. After the cells adhered to the wall, sensor CANQ and different concentrations of Zn<sup>2+</sup> ions were added to the cells and incubated. After the dishes were taken out, the medium was removed and washed three times with phosphate - buffered saline (PBS). The dishes were placed on the microscope to perform fluorescence confocal microscopic imaging to verify the practical properties of sensor CANQ in biological samples.

## 2 Results and discussion

### 2.1 Design and synthesis of sensor CANQ

The fluorescent sensor CANQ was designed by connecting 7-(*N,N*-diethylamino) coumarin-3-carbohydrazide and the unique properties of acenaphtho[1,2-*b*]quinoxaline-9-carbohydrazide. As shown in Scheme 1, sensor CANQ was synthesized by a simple Schiff base reaction, and the product was obtained as a yellow solid. The structure of intermediate and sensor CANQ was confirmed by <sup>1</sup>H NMR and MS spectra (Fig. S1-S10, Supporting information).

## 2.2 Optical response of CANQ toward Zn<sup>2+</sup>

The fluorescent spectra of sensor CANQ (5  $\mu\text{mol}\cdot\text{L}^{-1}$ ) were measured in a solution of  $\text{CH}_3\text{CH}_2\text{OH}/\text{Tris-HCl}$  (8:2,  $V/V$ ,  $\text{pH}=7.4$ ) at an excitation wavelength of 468 nm. Sensor CANQ itself had a weak fluorescent signal initially and the fluorescent emission was gradually enhanced at 522 nm with adding  $\text{Zn}^{2+}$  ion sequentially. As shown in Fig. 1, the sensor had a sensitive response to  $\text{Zn}^{2+}$  ions, and the fluorescence intensity titration curve reached a plateau after adding four equivalents  $\text{Zn}^{2+}$  ions<sup>[55-56]</sup>. To evaluate the binding ability of CANQ to  $\text{Zn}^{2+}$ , the binding constant based on the fluorescence intensity data was calculated<sup>[57]</sup> to be  $8.28\times 10^4 \text{ L}\cdot\text{mol}^{-1}$ , and some of the references recently published were taken to compare with this work (Table S1).

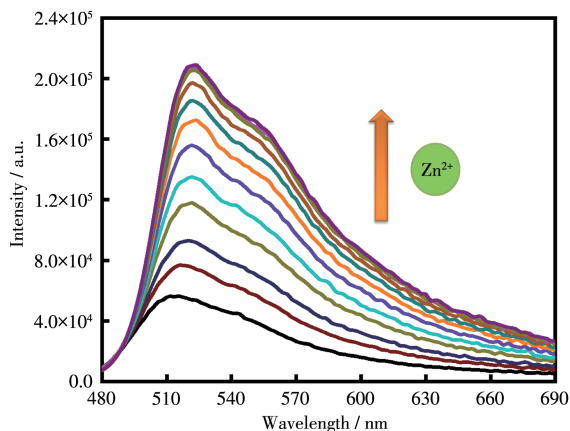


Fig. 1 Fluorescence spectra of CANQ with the addition of various concentrations of  $\text{Zn}^{2+}$  ion in  $\text{CH}_3\text{CH}_2\text{OH}/\text{Tris-HCl}$  (8:2,  $V/V$ ,  $\text{pH}=7.4$ ) solution

Interference of other metal ions directly affects the recognition of  $\text{Zn}^{2+}$  ions by the sensor in actual detection. So, the fluorescence response of sensor CANQ was monitored in the presence of 20  $\mu\text{mol}\cdot\text{L}^{-1}$  various metal ions ( $\text{Pb}^{2+}$ ,  $\text{Na}^+$ ,  $\text{Mn}^{2+}$ ,  $\text{Ca}^{2+}$ ,  $\text{Mg}^{2+}$ ,  $\text{Ag}^+$ ,  $\text{Cr}^{3+}$ ,  $\text{Fe}^{3+}$ ,  $\text{Fe}^{2+}$ ,  $\text{Hg}^{2+}$ ,  $\text{K}^+$ ,  $\text{Cd}^{2+}$ ,  $\text{Al}^{3+}$ ,  $\text{Cu}^{2+}$ ,  $\text{Zn}^{2+}$ ) in a mixed solution of  $\text{CH}_3\text{CH}_2\text{OH}/\text{Tris-HCl}$  (8:2,  $V/V$ ,  $\text{pH}=7.4$ ). As shown in Fig. 2, the enhancement of the fluorescence signal with the addition of other metal ions was weak and the fluorescence signal decreased slightly with adding the copper(II) ions. Sensor CANQ had considerable fluorescence enhancing with adding 20

$\mu\text{mol}\cdot\text{L}^{-1}$   $\text{Zn}^{2+}$  ion into the solution at 522 nm. These results reveal that sensor CANQ for detecting  $\text{Zn}^{2+}$  ion is of high selectivity and  $\text{Zn}^{2+}$  ion can be specifically identified without interference from other ions.

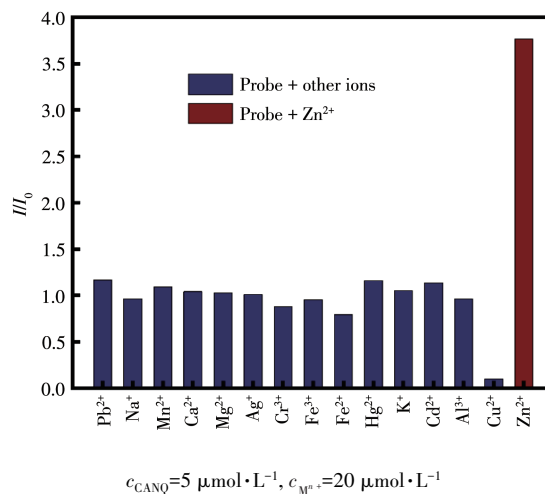


Fig. 2 Fluorescence response of sensor CANQ in the presence of various cations ( $\text{M}^{n+}$ ) in  $\text{CH}_3\text{CH}_2\text{OH}/\text{Tris-HCl}$  (8:2,  $V/V$ ,  $\text{pH}=7.4$ )

The good photostability of the fluorescent sensor is particularly important for the application of metal ions detection in the actual environment. As shown in Fig. 3, the fluorescent signal of sensor CANQ was stable within 10 min. After adding 20  $\mu\text{mol}\cdot\text{L}^{-1}$   $\text{Zn}^{2+}$  ion, the fluorescence signal of sensor CANQ enhanced fast, and the signal fluctuation was very weak within 10 min under room temperature. As illustrated in Fig.S11, in a wide pH range (from 4.5 to 9.4), the sensor CANQ had a significant fluorescence signal enhancement upon the addition of  $\text{Zn}^{2+}$  ions. These results reveal that the sen-

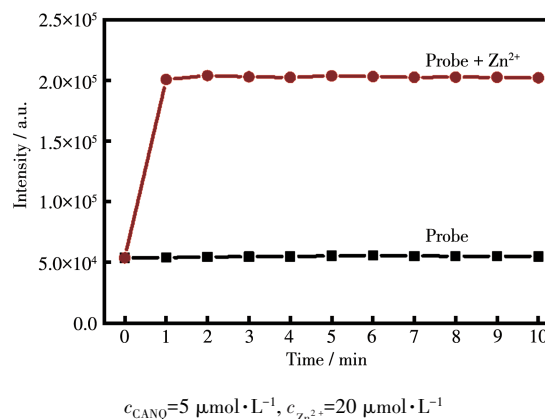


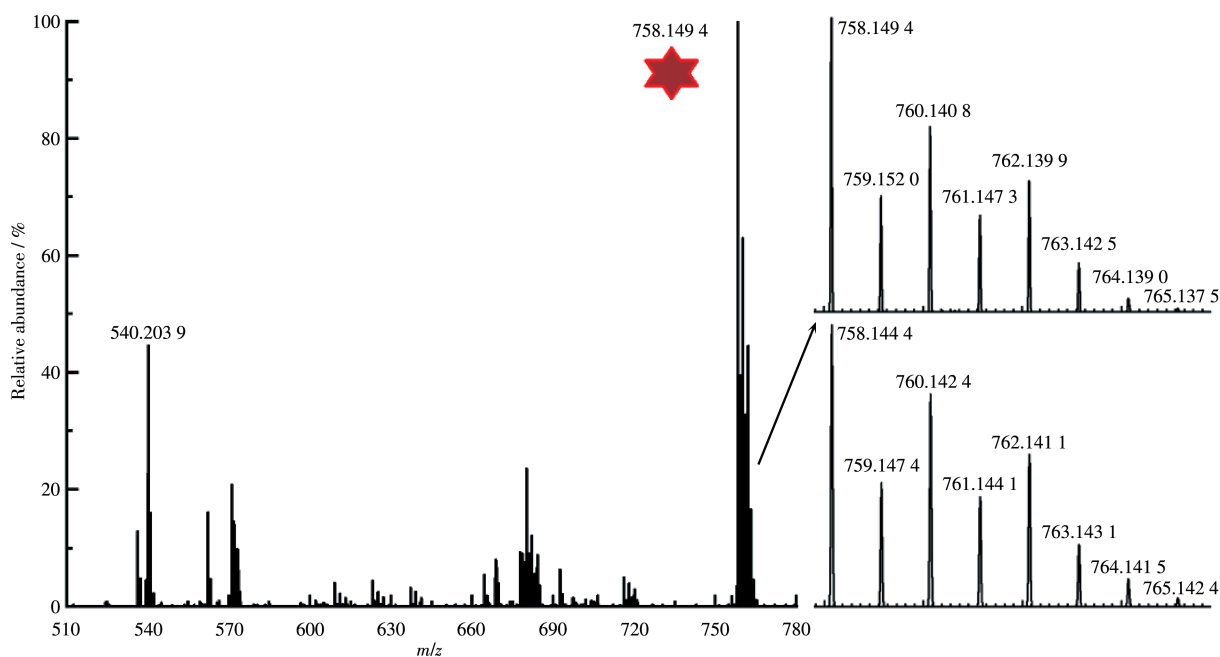
Fig. 3 Time-dependent fluorescent signal of sensor CANQ in the absence and presence of  $\text{Zn}^{2+}$  ion

sensor has a stable fluorescence response to  $Zn^{2+}$  ion and it is conducive to the detection of  $Zn^{2+}$  ion in the pH range of the physiological conditions.

### 2.3 Response mechanism

The high-resolution mass spectrum of the sensor before and after the addition of  $Zn^{2+}$  ions was recorded (Fig. 4). The intense peak  $m/z$  at 540.203 9 can be assigned to  $[CANQ+H]^+$ . The peak  $m/z$  at 758.149 4 was assigned to  $[CANQ-H+2DMSO+Zn]^+$  upon addi-

tion of  $Zn^{2+}$  ion, according to the comparison of the intense peak with the simulation-based on natural isotopic abundances (Inset of Fig. 4). This result indicates that a 1:1 stoichiometry complex was formed between  $Zn^{2+}$  and sensor CANQ, which was well consistent with the results of Job's plot (Fig. S12). This result can be inferred that sensor CANQ and  $Zn^{2+}$  ion can form coordination compounds<sup>[58-59]</sup> and interaction between them may lead to fluorescence signal enhancement.



Inset: experimental (top) and theoretical (bottom) MS peak of complex formed by sensor CANQ and  $Zn^{2+}$

Fig. 4 High-resolution mass spectrum of sensor CANQ in the presence of  $Zn^{2+}$  ion

### 2.4 Cytotoxicity

Furthermore, biosafety is indispensable for fluorescent sensors and their cytotoxicity and biocompati-

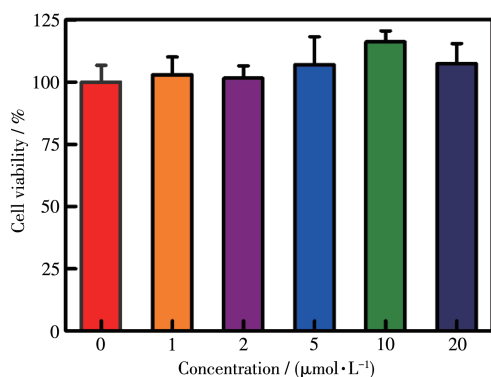


Fig. 5 Relative cell viability of MCF-7 cells incubated with different concentrations of sensor CANQ for 24 h estimated by CCK-8 assay

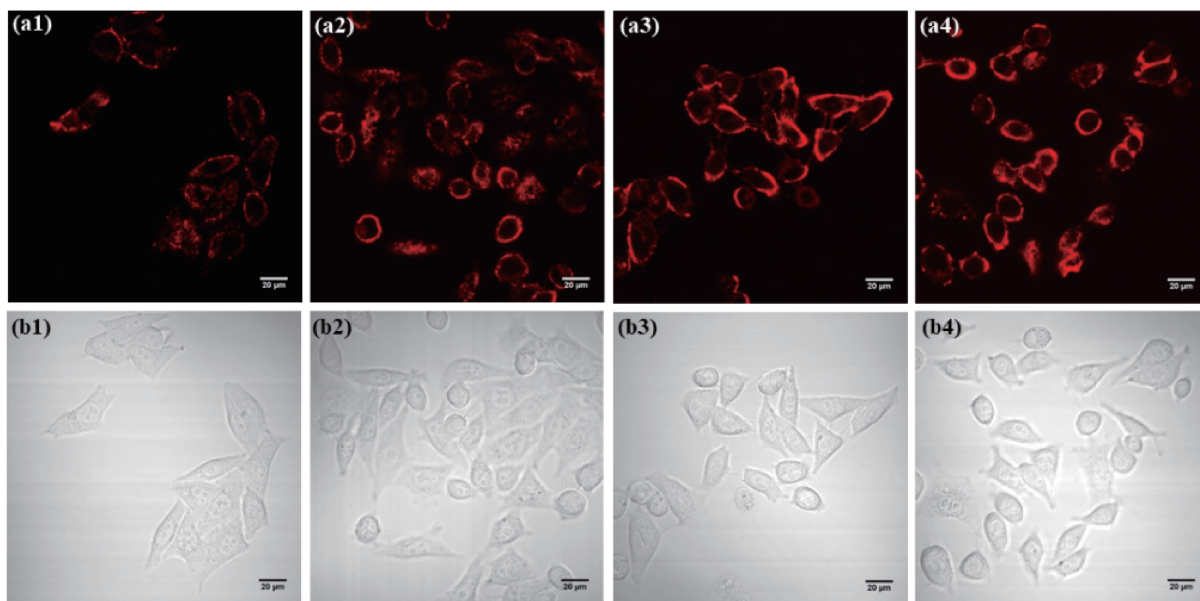
bility must be fully demonstrated before actual application. MCF-7 cells were incubated with different concentrations of sensor CANQ for 24 h, and the cytotoxicity was measured by CCK-8 reagent. When sensor CANQ concentration reached  $20 \mu\text{mol}\cdot\text{L}^{-1}$ , there wasn't significant fluctuation in the cell viability compared to the control group (Fig. 5). The results show that the synthesized sensor CANQ has very low cytotoxicity to cells and has excellent biocompatibility.

### 2.5 Confocal imaging

The ability of sensor CANQ to monitor the concentration of  $Zn^{2+}$  ions in living cells was determined, due to the fast and high selective fluorescence response. The MCF-7 cells were incubated with  $5 \mu\text{mol}\cdot\text{L}^{-1}$  sensor CANQ and were added varying concentrations of

Zn<sup>2+</sup> ion (0, 5, 10, and 20 μmol·L<sup>-1</sup>) for 20 min. After using the PBS to wash cells, fluorescence imaging experiments were performed with confocal laser scanning microscopy<sup>[60-61]</sup>. As shown in Fig.6, the cells that were incubated with sensor CANQ alone exhibited weak fluorescence response under the fluorescence channel, and cells treated with Zn<sup>2+</sup> ion showed obvious

fluorescence increasing. TPEN, which is a specific cell-permeable heavy metal chelator, effectively removed Zn<sup>2+</sup> ions in living MCF-7 cells incubated with Zn<sup>2+</sup> and sensor CANQ (Fig.S13), and the fluorescence signal of sensor CANQ decreased after adding TPEN. The results prove that sensor CANQ can be used for Zn<sup>2+</sup> ion imaging in living cells.



$c_{\text{CANQ}}=5 \mu\text{mol}\cdot\text{L}^{-1}$ ,  $c_{\text{Zn}^{2+}}=0 \mu\text{mol}\cdot\text{L}^{-1}$  (a1, b1),  $5 \mu\text{mol}\cdot\text{L}^{-1}$  (a2, b2),  $10 \mu\text{mol}\cdot\text{L}^{-1}$  (a3, b3),  $20 \mu\text{mol}\cdot\text{L}^{-1}$  (a4, b4),  $\lambda_{\text{ex}}=458 \text{ nm}$ ,  $\lambda_{\text{em}}=480\text{-}580 \text{ nm}$

Fig.6 Fluorescence confocal microscopy images of MCF-7 cells incubated with sensor CANQ and Zn<sup>2+</sup> ion with different concentrations: (a1-a4) fluorescent images; (b1-b4) bright-field microscopic images

### 3 Conclusions

In conclusion, a novel fluorescent sensor CANQ based on coumarin derivative was designed and synthesized. CANQ was used to recognize Zn<sup>2+</sup> ions by fluorescence enhancement in a mixed solution of CH<sub>3</sub>CH<sub>2</sub>OH/Tris-HCl (8:2, V/V, pH=7.4). The fluorescent emission was significantly increased at 522 nm after adding Zn<sup>2+</sup> ions. Sensor CANQ can selectively detect Zn<sup>2+</sup> among various relevant metal ions and has good photostability. Sensor CANQ also has excellent biocompatibility, and it has been successfully applied to fluorescence confocal microscopic imaging of MCF-7 cells, which provides reference experience for the detection of Zn<sup>2+</sup> ions in biological analysis.

**Acknowledgments:** We acknowledge SI Wen, GAO Xu, ZUO Ying-Ying for their aid in this work.

Supporting information is available at <http://www.wjhxsb.cn>

### References:

- [1]Tang L J, Xia J Y, Zhong K L, Tang Y W, Gao X, Li J R. A Simple AIE-Active Fluorogen for Relay Recognition of Cu<sup>2+</sup> and Pyrophosphate through Aggregation-Switching Strategy. *Dyes Pigm.*, **2020**,**178**: 108379
- [2]Chasapis C T, Ntoupa P S A, Spiliopoulou C A, Stefanidou M E. Recent Aspects of the Effects of Zinc on Human Health. *Arch. Toxicol.*, **2020**, **94**:1443-1460
- [3]Chang Y X, Li B, Mei H H, Xu K X, Xie X M, Yang L. A Novel Reversible Fluorescent Probe for Zinc(II) Ion and Bioimaging in Living Cells. *Supramol. Chem.*, **2020**,**32**:93-402
- [4]Pluth M D, Tomat E, Lippard S J. Biochemistry of Mobile Zinc and Nitric Oxide Revealed by Fluorescent Sensors. *Annu. Rev. Biochem.*, **2011**,**80**:333-355
- [5]Aydin D. A Novel Turn On Fluorescent Probe for the Determination of Al<sup>3+</sup> and Zn<sup>2+</sup> Ions and its Cells Applications. *Talanta*, **2020**, **210**: 120615

- [6]Kang T T, Wang H P, Wang X J, Feng L H. A Facile Zn(II) Probe Based on Intramolecular Charge Transfer with Fluorescence Red-Shift. *Microchem. J.*, **2019**,**148**:442-448
- [7]Lin L Y, Hu Y F, Zhang L L, Huang Y, Zhao S L. Photoluminescence Light-Up Detection of Zinc Ion and Imaging in Living Cells Based on the Aggregation Induced Emission Enhancement of Glutathione-capped Copper Nanoclusters. *Biosens. Bioelectron.*, **2017**,**94**:523-529
- [8]Shang Y F, Wang H L, Bai H. A Coumarin-Based Turn-On Chemosensor for Selective Detection of Zn(II) and Application in Live Cell Imaging. *Spectrochim. Acta Part A*, **2020**,**228**:117746
- [9]Frederickson C J, Koh J Y, Bush A I. The Neurobiology of Zinc in Health and Disease. *Nat. Rev. Neurosci.*, **2005**,**6**:449-462
- [10]Lippi S L P, Kakalec P A, Smith M L, Flinn J M. Wheel-Running Behavior is Negatively Impacted by Zinc Administration in a Novel Dual Transgenic Mouse Model of AD. *Front. Neurosci.*, **2020**,**14**:854
- [11]Fang M X, Xia S, Bi J H, Wigstrom T P, Valenzano L, Wang J B, Tanasova M, Luck R L, Liu H Y. Detecting Zn(II) Ions in Live Cells with Near-Infrared Fluorescent Probes. *Molecules*, **2019**,**24**:1592
- [12]Kwon N, Hu Y, Yoon J. Fluorescent Chemosensors for Various Analytes Including Reactive Oxygen Species, Biothiol, Metal Ions, and Toxic Gases. *ACS Omega*, **2018**,**3**:13731-13751
- [13]Prasad A S. Discovery of Human Zinc Deficiency: Its Impact on Human Health and Disease. *Adv. Nutr.*, **2013**,**4**:176-190
- [14]Pohl P. Determination of Metal Content in Honey by Atomic Absorption and Emission Spectrometries. *TrAC-Trend Anal. Chem.*, **2009**,**28**:117-128
- [15]Silva E L, Roldan P D S, Gine M F. Simultaneous Preconcentration of Copper, Zinc, Cadmium, and Nickel in Water Samples by Cloud Point Extraction Using 4-(2-Pyridylazo)-resorcinol and Their Determination by Inductively Coupled Plasma Optic Emission Spectrometry. *J. Hazard. Mater.*, **2009**,**171**:1133-1138
- [16]Murugan A S, Vidhyalakshmi N, Ramesh U, Annaraj J. A Schiff's Base Receptor for Red Fluorescence Live Cell Imaging of Zn<sup>2+</sup> Ions in Zebrafish Embryos and Naked Eye Detection of Ni<sup>2+</sup> Ions for Bio-Analytical Applications. *J. Mater. Chem. B*, **2017**,**5**:3195-3200
- [17]Khun N W, Liu E. Linear Sweep Anodic Stripping Voltammetry of Heavy Metals from Nitrogen Doped Tetrahedral Amorphous Carbon Thin Films. *Electrochim. Acta*, **2009**,**54**:2890-2898
- [18]Li W Y, Fang B Q, Jin M, Tian Y. Two-Photon Ratiometric Fluorescence Probe with Enhanced Absorption Cross Section for Imaging and Biosensing of Zinc Ions in Hippocampal Tissue and Zebrafish. *Anal. Chem.*, **2017**,**89**:2553-2560
- [19]Zhang S W, Adhikari R, Fang M X, Dorh N, Li C, Jaishi M, Zhang J T, Tiwari A, Pati R, Luo F T, Liu H Y. Near-Infrared Fluorescent Probes with Large Stokes Shifts for Sensing Zn(II) Ions in Living Cells. *ACS Sens.*, **2016**,**1**:1408-1415
- [20]Yan L Q, Li R J, Ma F L, Qi Z J. A Simple Salicylaldehyde-Based Fluorescent "Turn-On" Probe for Selective Detection of Zn<sup>2+</sup> in Water Solution and Its Application in Live Cell Imaging. *Anal. Methods*, **2017**,**9**:1119-1124
- [21]Gan X P, Sun P, Li H, Tian X H, Zhang B W, Wu J Y, Tian Y P, Zhou H P. A Conveniently Prepared and Hypersensitized Small Molecular Fluorescent Probe: Rapidly Detecting Free Zinc Ion in HepG2 Cells and Arabidopsis. *Biosens. Bioelectron.*, **2016**,**86**:393-397
- [22]Kumar M, Kumar A, Singh M K, Sahu S K, John R P. A Novel Benzidine Based Schiff Base "Turn-On" Fluorescent Chemosensor for Selective Recognition of Zn<sup>2+</sup>. *Sens. Actuators B*, **2017**,**241**:1218-1223
- [23]Jiang G R, Shi F, Jia Y M, Cui S Q, Pu S Z. A Novel Donor-Acceptor Fluorescent Sensor for Zn<sup>2+</sup> with High Selectivity and Its Application in Test Paper. *J. Fluoresc.*, **2020**,**30**:1567-1574
- [24]Turnbull W L, Luyt L G. Amino-Substituted 2,2'-Bipyridine Ligands as Fluorescent Indicators for Zn<sup>II</sup> and Applications for Fluorescence Imaging of Prostate Cells. *Chem. Eur. J.*, **2018**,**24**:14539-14546
- [25]Ojida A, Sakamoto T, Inoue M, Fujishima S, Lippens G, Hamachi I. Fluorescent BODIPY-Based Zn(II) Complex as a Molecular Probe for Selective Detection of Neurofibrillary Tangles in the Brains of Alzheimer's Disease Patients. *J. Am. Chem. Soc.*, **2009**,**131**:6543-6548
- [26]Xue J, Tian L M, Yang Z Y. A Novel Rhodamine-Chromone Schiff-Base as Turn-On Fluorescent Probe for the Detection of Zn(II) and Fe(III) in Different Solutions. *J. Photochem. Photobiol. A*, **2019**,**369**:77-84
- [27]Han Z X, Zhang X B, Zhuo L, Gong Y J, Wu X Y, Jin Z, He C M, Jian L X, Zhang J, Shen G L, Yu R Q. Efficient Fluorescence Resonance Energy Transfer-Based Ratiometric Fluorescent Cellular Imaging Probe for Zn<sup>2+</sup> Using a Rhodamine Spirolactam as a Trigger. *Anal. Chem.*, **2010**,**82**:3108-3113
- [28]Yoon S A, Lee J, Lee M H. A Ratiometric Fluorescent Probe for Zn<sup>2+</sup> Based on Pyrene-Appendednaphthalimide-Dipicolylamine. *Sens. Actuators B*, **2018**,**258**:50-55
- [29]Tian X H, Hussain S, de Pace C, Ruiz-Perez L, Battaglia G. Zn<sup>II</sup> Complexes for Bioimaging and Correlated Applications. *Chem. Asian J.*, **2019**,**14**:509-526
- [30]Xie G Q, Shi Y J, Hou F P, Liu H Y, Huang L, Xi P X, Chen F J, Zeng Z Z. A Highly Selective Fluorescent and Colorimetric Chemosensor for Zn<sup>II</sup> and Its Application in Cell Imaging. *Eur. J. Inorg. Chem.*, **2012**:327-332
- [31]Che W L, Yu T C, Jin D, Ren X Y, Zhu D X, Su Z M, Bryce M R. A Simple Oxazoline as Fluorescent Sensor for Zn<sup>2+</sup> in Aqueous Media. *Inorg. Chem. Commun.*, **2016**,**69**:89-93
- [32]Cao D X, Liu Z Q, Verwilt P, Koo S, Jangjili P, Kim J S, Lin W Y. Coumarin-Based Small-Molecule Fluorescent Chemosensors. *Chem. Rev.*, **2019**,**119**:10403-10519
- [33]Geißler D, Antonenko Y N, Schmidt R, Keller S, Krylova O O, Wiesner B, Bendig J, Pohl P, Hagen V. (Coumarin-4-yl)methyl Esters as Highly Efficient, Ultrafast Phototriggers for Protons and Their Application to Acidifying Membrane Surfaces. *Angew. Chem. Int. Ed.*, **2005**,**44**:1195-1198
- [34]Xu Z C, Liu X, Pan J, Spring D R. Coumarin-Derived Transformable Fluorescent Sensor for Zn<sup>2+</sup>. *Chem. Commun.*, **2012**,**48**:4764-4766

- [35] Bhattacharyya A, Makhal S C, Guchhait N. Evaluating the Merit of a Diethylamino Coumarinderived Thiosemicarbazone as an Intramolecular Charge Transfer Probe: Efficient Zn (II) Mediated Emission Swing from Green to Yellow. *Photochem. Photobiol. Sci.*, **2019**, **18**: 2031-2041
- [36] Feng S, Gao Q M, Gao X, Yin J Q, Jiao Y. Fluorescent Sensor for Copper(II) Ions Based on Coumarin Derivative and Its Application in Cell Imaging. *Inorg. Chem. Commun.*, **2019**, **102**:51-56
- [37] Mani K S, Rajamanikandan R, Murugesapandian B, Shankar R, Sivaraman G, Ilanchelian M, Rajendran S P. Coumarin Based Hydrazone as an ICT-Based Fluorescence Chemosensor for the Detection of Cu<sup>2+</sup> Ions and the Application in HeLa Cells. *Spectrochim. Acta Part A*, **2019**, **214**:170-176
- [38] Dai X, Zhang T, Du Z F, Cao X J, Chen M Y, Hu S W, Miao J Y, Zhao B X. An Effective Colorimetric and Ratiometric Fluorescent Probe for Bisulfite in Aqueous Solution. *Anal. Chim. Acta*, **2015**, **888**: 138-145
- [39] Li M X, Feng W Y, Zhang H Y, Feng G Q. An Aza-Coumarin-Hemicyanine Based Near-Infrared Fluorescent Probe for Rapid, Colorimetric and Ratiometric Detection of Bisulfite in Food and Living Cells. *Sens. Actuators B*, **2017**, **243**:51-58
- [40] Zhou X, Kwon Y, Kim G, Ryu J H, Yoon J. A Ratiometric Fluorescent Probe Based On a Coumarin-Hemicyanine Scaffold for Sensitive and Selective Detection of Endogenous Peroxynitrite. *Biosens. Bioelectron.*, **2015**, **64**:285-291
- [41] Wu W L, Zhao X, Xi L L, Huang M F, Zeng W H, Miao J Y, Zhao B X. A Mitochondria - Targeted Fluorescence Probe for Ratiometric Detection of Endogenous Hypochlorite in the Living Cells. *Anal. Chim. Acta*, **2017**, **950**:178-183
- [42] Ghosh A C, Weisz K, Schulzke C. Selective Capture of Ni<sup>2+</sup> Ions by Naphthalene- and Coumarin-Substituted Dithiolenes. *Eur. J. Inorg. Chem.*, **2016**:208-218
- [43] Maity S B, Bharadwaj P K. A Molecular Dual Fluorescence - ON Probe for Mg<sup>2+</sup> and Zn<sup>2+</sup>: Higher Selectivity towards Mg<sup>2+</sup> over Zn<sup>2+</sup> in a Mixture. *J. Lumin.*, **2014**, **155**:21-26
- [44] Jonaghani M Z, Zali-Boeini H, Moradi H. A Coumarin Based Highly Sensitive Fluorescent Chemosensor for Selective Detection of Zinc Ion. *Spectrochim. Acta Part A*, **2019**, **207**:16-22
- [45] Albratty M, El-Sharkawy K A, Alam S. Synthesis and Antitumor Activity of Some Novel Thiophene, Pyrimidine, Coumarin, Pyrazole and Pyridine Derivatives. *Acta Pharm.*, **2017**, **67**:15-33
- [46] Jorge E G, Rayar A M, Barigye S J, Rodriguez M E J, Veitia M S I. Development of an *In Silico* Model of DPPH Free Radical Scavenging Capacity: Prediction of Antioxidant Activity of Coumarin Type Compounds. *Int. J. Mol. Sci.*, **2016**, **17**:881
- [47] Wang Y B, Liu H T, Lu P, Mao R, Xue X J, Fan C, She J X. Design, Synthesis, and *In Vitro* Evaluation of Novel 3,7-Disubstituted Coumarin Derivatives as Potent Anticancer Agents. *Chem. Biol. Drug Des.*, **2015**, **86**:637-647
- [48] Hasaninejad A, Zare A, Mohammadzadeh M R, Shekouhy M. Lithium Bromide as an Efficient, Green, and Inexpensive Catalyst for the Synthesis of Quinoxaline Derivatives at Room Temperature. *Green Chem. Lett. Rev.*, **2010**, **3**:143-148
- [49] Elmes R B P. Bioreductive Fluorescent Imaging Agents: Applications to Tumour Hypoxia. *Chem. Commun.*, **2016**, **52**:8935-8956
- [50] Zhang H, Fan J L, Wang J Y, Zhang S Z, Dou B R, Peng X J. An Off-On COX-2-Specific Fluorescent Probe: Targeting the Golgi Apparatus of Cancer Cells. *J. Am. Chem. Soc.*, **2013**, **135**:11663-11669
- [51] Zhang T, Yin C X, Zhang Y B, Chao J B, Wen G M, Huo F J. Mitochondria - Targeted Reversible Ratiometric Fluorescent Probe for Monitoring SO<sub>2</sub>/HCHO in Living Cells. *Spectrochim. Acta Part A*, **2020**, **234**:118253
- [52] Renault K, Renard P Y, Sabot C. Detection of Biotinols with a Fast-Responsive and Water-Soluble Pyrazolone-Based Fluorogenic Probe. *Eur. J. Org. Chem.*, **2018**, **46**:6494-6498
- [53] Mahjoob E., Khalaj A, Ostad S N, Azizi E., Fouladdel S, Tavajohi S, Salehi R, Dowlatabadi R. Investigation of Selective Cytotoxicity and Determination of Ligand Induced Apoptosis of a New Acenaphtho[1,2-*b*]quinoxaline Derivative. *Arzneimittelforschung*, **2009**, **59**:526-531
- [54] Lin K T, Lai C K. Phase Crossover in Columnar Tris-(1,3,4-oxadiazoles) with Pendant Quinoxalines. *Tetrahedron*, **2016**, **72**:7579-7588
- [55] Kim M S, Jo T G, Yang M, Han J, Lim M H, Kim C. A Fluorescent and Colorimetric Schiff Base Chemosensor for the Detection of Zn<sup>2+</sup> and Cu<sup>2+</sup>: Application in Live Cell Imaging and Colorimetric Test Kit. *Spectrochim. Acta Part A*, **2019**, **211**:34-43
- [56] Roy A, Shee U, Mukherjee A, Mandal S K, Roy P. Rhodamine - Based Dual Chemosensor for Al<sup>3+</sup> and Zn<sup>2+</sup> Ions with Distinctly Separated Excitation and Emission Wavelengths. *ACS Omega*, **2019**, **4**: 6864-6875
- [57] Dey S, Halder S, Mukherjee A, Ghosh K, Roy P. Development of Highly Selective Chemosensor for Al<sup>3+</sup>: Effect of Substituent and Biological Application. *Sens. Actuators B*, **2015**, **215**:196-205
- [58] Ahamed B N, Ghosh P. A Chelation Enhanced Selective Fluorescence Sensing of Hg<sup>2+</sup> by a Simple Quinoline Substituted Tripodal Amide Receptor. *Dalton Trans.*, **2011**, **40**:12540-12547
- [59] Zhang Y P, Xue Q H, Yang Y S, Liu X Y, Ma C M, Ru J X, Guo H C. A Chromene Pyrazoline Derivatives Fluorescent Probe for Zn<sup>2+</sup> Detection in Aqueous Solution and Living Cells. *Inorg. Chim. Acta*, **2018**, **479**:128-134
- [60] Huo F J, Wu Q, Kang J, Zhang Y B, Yin C X. A Specific Fluorescent Probe for Zinc Ion Based on Thymolphthalein and Its Application in Living Cells. *Sens. Actuators B*, **2018**, **262**:263-269
- [61] Wang P, Wu J. A Highly Sensitive Turn-On Fluorescent Chemosensor for Recognition of Zn(II) Ions and Its Application in Live Cells Imaging. *J. Photochem. Photobiol. A*, **2020**, **386**:112111